Design and Fabrication of a Magnetic Propulsion System for Self-Propelled Capsule Endoscope

Article *in* IEEE transactions on bio-medical engineering · December 2010

DOI: 10.1109/TBME.2010.2051947 · Source: PubMed

Design and Fabrication of a Magnetic Propulsion System for Self-Propelled Capsule Endoscope

Mingyuan Gao, *Student Member, IEEE*, Chengzhi Hu, Zhenzhi Chen, Honghai Zhang, and Sheng Liu*, *Senior Member, IEEE*

***Abstract*—This paper investigates design, modeling, simulation, and control issues related to self-propelled endoscopic capsule navigated inside the human body through external magnetic fields. A novel magnetic propulsion system is proposed and fabricated, which has great potential of being used in the field of noninvasive gastrointestinal endoscopy. Magnetic-analysis model is established and finite-element simulations as well as orthogonal design are performed for obtaining optimized mechanical and control parameters for generating appropriate external magnetic field. Simulated intestinal tract experiments are conducted, demonstrating controllable movement of the capsule under the developed magnetic propulsion system.**

***Index Terms*—Biomedical equipment, capsule endoscope, gastrointestinal (GI) endoscopy, magnetic propulsion, orthogonal process design.**

I. Introduction

OVER 3 million people annually in the U.S. alone suffer gastrointestinal (GI) disease serious enough to require hospitalization and 300 000 people die from GI diseases annually in China [1]–[3]. Recently, commercialized passive-controlled wireless capsule endoscopy, which had been developed since 2000, exploits a swallowable capsule endoscope that includes digital camera, application-specified integrated circuit (ASIC) transmitter, antenna, illuminating LED-assisted imaging, and battery for access to the GI tract [1], [4]. Capsule endoscope with the size of a normal pill can be easily swallowed by patients of various ages. It takes pictures throughout the GI tract by sending images to an external recorder, and thus provides useful information for clinic diagnosis of GI tract diseases (as shown in Fig. 1).

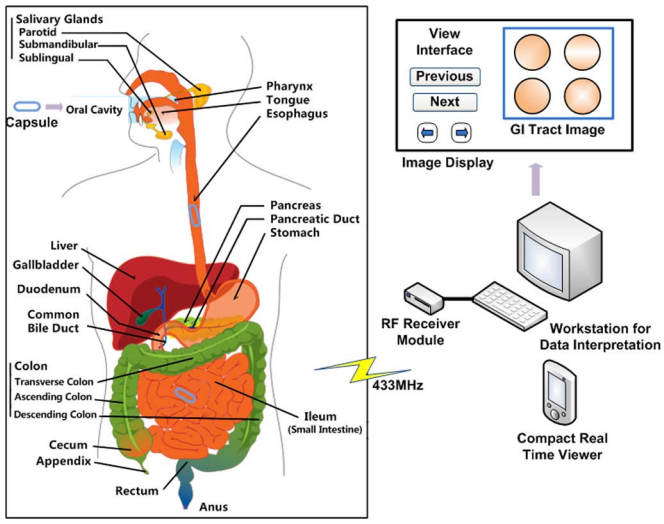

Fig. 1. Background of capsule endoscopy (GI tract image was from [34]).

Although capsule endoscopy has achieved great progress compared to traditional invasive endoscopy, it still has many limitations [5]–[7]. With the development of electronics, microsystems fabrication, and wireless communication technology, research and progress on a self-propelled capsule endoscope have been the topic of interests for several years [8]–[11]. A wide variety of active and wireless control mechanisms have been developed for self-propelled endoscopic capsule such as shape memory alloy (SMA) actuator, spiral-type micromachine, electrical stimulus capsule, motor-legged robot, and hydraulic manipulator [12]–[33].

Ishiyama *et al.* in Tohoku University proposed one type of micromachine with an inside permanent magnet and a spiral structure [12]–[14]. The micromachine was rotated and propelled by applying an external rotational magnetic field, which was generated by three pairs of Helmholtz coils. They had reported corresponding experiments both *in vivo* and *in vitro*, demonstrating feasibilities of the rotating magnetic guidance system [15], [16]. However, due to safety issues of electromagnetic radiation induced by low-frequency magnetic field and inaccessibility of the spiral-based capsule to the stomach, application of this technique is still limited in minimally invasive therapy of human body.

Manuscript received January 7, 2010; revised April 1, 2010; accepted May 25, 2010. Date of publication June 10, 2010; date of current version November 17, 2010. This work was supported by the National High Technology Research and Development Program of China under the Ministry of Science and Technology under Program 863 (no. 2008AA04Z313). The work of M. Gao and C. Hu was supported by the Graduate Innovation Foundation Program from the Huazhong University of Science and Technology (no. HF0601108100). M. Gao and C. Hu equally contributing co-first authors. *Asterisk indicates corresponding author.*

M. Gao was with the School of Mechanical Science and Engineering, Huazhong University of Science and Technology, Wuhan 430074, China. He is now with the Micro Energy System Lab., the University of Tokyo, Japan (e-mail: goalmychn@gmail.com).

C. Hu was with the School of Mechanical Science and Engineering, Huazhong University of Science and Technology, Wuhan 430074, China. He is now with Nagoya University, Nagoya 464-8601, Japan (e-mail: huzhiming_hcz@126.com).

Z. Chen and H. Zhang are with the School of Mechanical Science and Engineering, Huazhong University of Science and Technology, Wuhan 430074, China (e-mail: airender@163.com; honghaizhang@tom.com).

*S. Liu is with the School of Mechanical Science and Engineering, and the National Laboratory for Optoelectronics, Huazhong University of Science and Technology, Wuhan 430074, China (e-mail: victor_liu63@126.com).

Color versions of one or more of the figures in this paper are available online at http://ieeexplore.ieee.org.

Digital Object Identifier 10.1109/TBME.2010.2051947

TABLE I
ACTIVE LOCOMOTION APPROACHES OF CAPSULE ENDOSCOPY

Approaches	Electrical Stimulation Capsule	Earthworm	Shape Memory Alloy	Spiral-blade Capsule	Magnetic Control System	Legged Locomotion Robot	Magnetic Shell Navigation
Research Groups	Royal London Hospital	MiT Lab, Scuola Superiore Sant'Anna	Micro-systems Center, Institute of Sci.&Tech., Seoul	Ishiyama Laboratory, Tohoku University	College of Electrical Engineering, NTU	MiT Lab, Scuola Superiore Sant'Anna	Interdepartmental Research Centre, University of Pisa
Checked Site	Small Intestine	Colon	Small Intestine	Small & Big Bowel	Small & Big Bowel	Small & Big Bowel	GI Tract
Capsule Size	ø15- ø23mm	ø18×50(80)mm[i]	ø13×33mm	ø11×40mm	ø11×26mm	ø12×40mm	ø11×26mm
Locomotion Speed	4.5-6mm/s	1.5-5mm/s	0.142-0.245 mm/s	5-10mm/s	5-10mm/s	0.2-0.5mm/s	1-10 mm/s [ii]
Driving Force	0.3-0.6N	5N(max)	1.36N	1.5-3.0mNm	1.5-3.0mNm	1.0-2.0N	0.1-5N[iii]
Locomotion Principle	Electro-physiology	Biomimetics	SMA Effect	Rotating Magnetic Field & Spiral Structure	Rotating Magnetic Field & Spiral Structure	Biomimetics	Static Magnetic Field Propulsion
Control Method	Cable	Cable	Cable	Wireless	Wireless	Cable	Wireless
Power Consumption	9-12mW	800mW	500-800mW	10-20mW	5-20mW	200mW	10mW
Space for Outside Devices	Little	Little	Little	Big	Moderate	Little	Big
Harm to GI Tract	Little	Moderate	Great	Great	Great	Little	Little
Potential Safety Hazard	Unknown Effect on Peristalsis	Bellow Effect	High Temperature	Electromagnetic Radiation	Little	Robot Legs' Retention in Body	Little

[i] The length of micro robot is 50 mm in retraction and 80 mm in elongation;
[ii] Capsule's locomotion speed depends on the location and orientation of outside magnetic propulsion equipment;
[iii] With the increase of the distance, the magnitude of magnetic force drops rapidly.

Kim *et al.* developed a locomotion mechanism for endoscopic capsule using SMAs [17]. Prototype endoscopes including four pairs of SMA springs and clampers were fabricated, and *in vitro* tests confirmed that the device was able to move in the tract with a speed of 9.19 mm/min at a current of 300 mA when controlling the four pieces of the moving modules sequentially. However, considering issues of great power consumption and high operation temperature associated with SMA-based microrobot, state-of-the-art power-generation technology is expected to be developed for substituting the currently commercial battery for this specific application.

Mosse *et al.* proposed an electrical simulation method for propelling an endoscope in the small intestine [18]. The locomotion principle is that, by electro-stimulating circle muscle contraction of the intestinal wall, the device can be propelled forwardly or backwardly. Five devices with a diameter ranging from 15 to 23 and with a taper of 28–40 degrees were tested in the small intestine and esophagus of anesthetized pigs. When stimulated at 15 Hz with 30-ms pulses at 20 mA, the device moved reliably in either direction in the small intestine at a maximum speed of 4.5 mm/s and negotiated tight curves. Electrical stimulus approach has an unknown effect to the peristalsis mechanism of the intestine. Further research needs to be carried out for inspecting this electrophysiological problem.

Dario's research group proposed an actuation mechanism exploiting a legged microrobot to perform active exploration of the digestive tract [19]–[22]. This device is equipped with four super elastic legs, allowing large stroke advancement in the GI tract, and a CMOS frontal camera to visualize the intestinal wall. Preliminary experimental results *in vitro* demonstrated that the device was capable of traveling in the digestive tract with a typical speed ranging between 10 and 40 mm/min.

Carpi *et al.* at the University of Pisa developed a solution using an external magnetic field applied to the endoscopic capsule, thus providing an approach of controlling capsule's location previously coated with a magnetic shell [24]–[26]. This technique, on the one hand, can interact with an imposed external magnetic field in the GI tract; on the other hand, it is readily and cheaply compatible with currently commercialized capsule endoscope, and thus needs no modification of internal configuration. Recently, they used a commercial computer-aided surgery system (Niobe, Stereotaxis, St. Louis, MO) as the controllable source of magnetic field. They have reported the feasibility of using the technology of magnetic navigation in the field of GI endoscopy, and preliminary proof-of-concept investigations have been performed [25]. However, The Stereotaxis is an advanced cardiology system for use in the cardiac catheterization. Thus, a navigation system should be designed for negotiating the specific application of GI endoscopy. At present, to the best of our knowledge, few automated magnetic navigation systems have been proposed and fabricated for serving the patients in the field of noninvasive GI endoscopy due to many concerns such as safety and cost (Table I is a review of current active locomotion approaches of capsule endoscopy).

Based on these motivations, we proposed an automated multiaxis magnetic propulsion system for specific application of controlling the endoscopic capsule's location and orientation in the GI tract. Magnetic-analysis model was established and

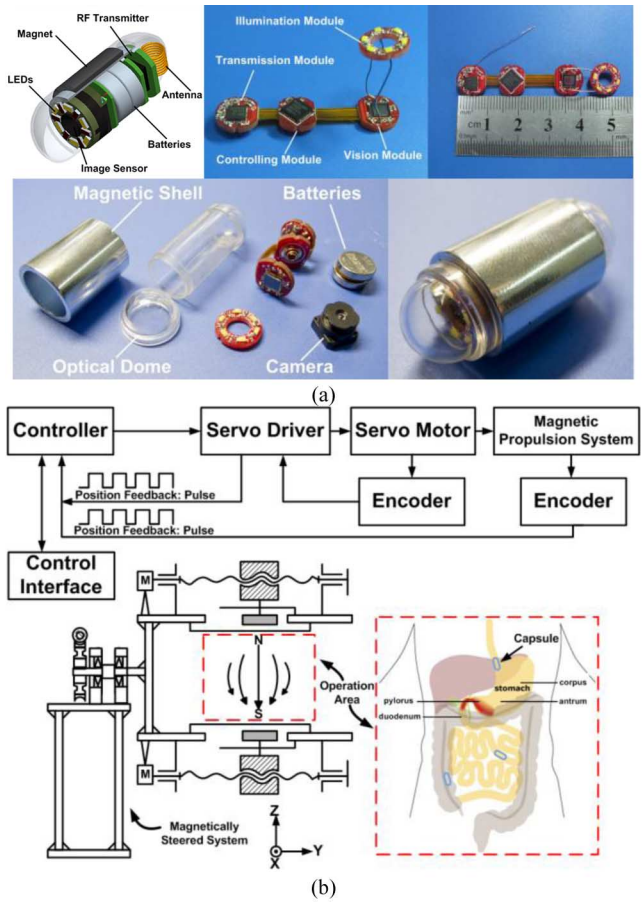

Fig. 2. Engineering design of the magnetic propelled endoscopic system. (a) Illumination module, vision module, controlling module, and wireless transmission module are related through flexible connection. The overall dimensions of the device are 12 mm × 34 mm (without magnetic shell). (b) Schematic diagram showing operation flow of the magnetic propulsion system.

finite-element (FE) method was developed for obtaining optimized mechanical and control parameters for generating appropriate external magnetic field. In order to judge the feasibility of the proposed system, experimental tests were carried out and it demonstrated controlled translations and rotations of the capsule under this novel propulsion system.

II. System Design and Locomotion Analysis

In this study, we focus on the design and integration of a magnetic propulsion system for specific application of active locomotion control of the endoscopic capsule in the GI tract. Engineering design of the magnetic propelled endoscopic system is summarized in Fig. 2.

A. Wireless Capsule Endoscope

The developed endoscopic capsule is constructed by four main parts—illumination module, vision module, controlling module, and wireless transmission module, as shown in Fig. 2(a). The concept of the magnetic shell is proposed by Carpi *et al.* [24]–[26]. The microsystems integration of the capsule endoscope is based on commercialized chips and devices available on the markets, thereby rendering the total costs of

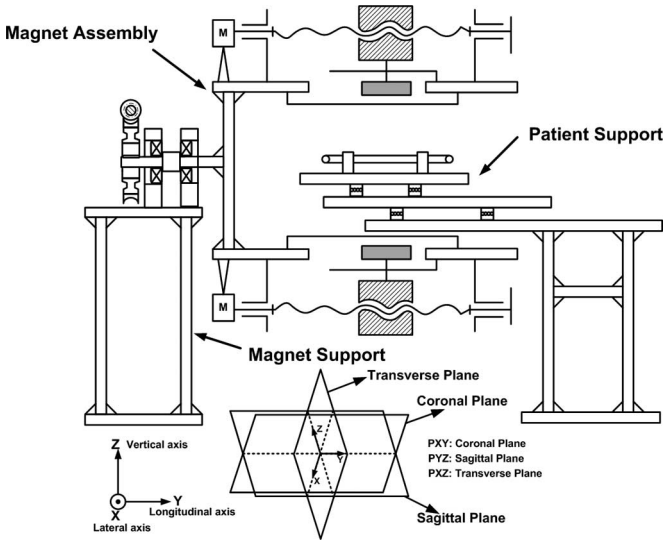

Fig. 3. Overall assembly drawing of magnetic propulsion system.

the endoscopic capsule less than 5 dollars and dimension of ø12 mm × 34 mm (without magnetic shell). In this paper, we mainly focus on discussion of the developed magnetic propulsion system as follows.

B. Magnetic Propulsion System

Fig. 3 illustrates the assembly drawing of magnetic propulsion system. The patient support, which can be moved along the longitudinal direction forwardly and rearwardly and along the lateral direction inwardly and outwardly, is mounted on a pedestal, allowing the patient to be moved relative to the magnet assembly. The magnet assembly comprises several Nd–Fe–B permanent magnets, ball screws, linear ball rails, and gripper device. The ball screws convert motor's rotary motion to ball nut's linear motion, exerting necessary force to move the permanent magnets along a longitudinal axis. Once the two groups of oppositely positioned magnets are moved in the opposite direction parallel to the longitudinal axis, the magnet inside the capsule endoscope will be rotated about its lateral or vertical axis or any axis in the transverse plane according to the different positions of magnet support. The magnet support contains a pair of worm/worm gear, a pivot, and aluminum framing. The magnet assembly is mounted onto the magnet support and can rotate about the longitudinal axis. The relative rotation between magnet assembly and patient support permits adjustment of the positions of magnet, allowing magnet built-in capsule endoscope to rotate about its longitudinal axis. According to the position feedback information, the servo control unit gives orders for driving the multiaxes of the magnetic propulsion system. Position control mode with pulse signal input is adopted and human–machine interface is developed for realizing semiautomatic control. During the operation procedure, input control parameters should be amended artificially for realizing the stable movements of the capsule [see Fig. 2(b)].

The proposed magnetic propulsion system has five coupling axes that can realize capsule endoscope's multidirection movement in the GI tract. Fig. 4 demonstrates the principle of capsule

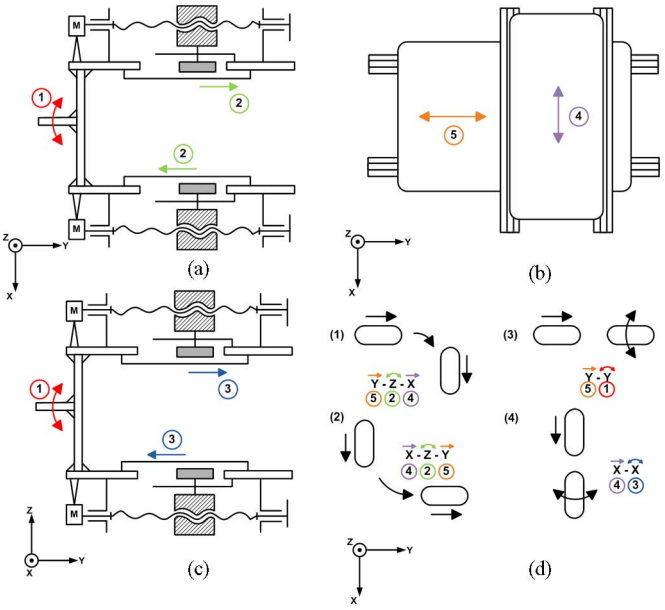

Fig. 4. Locomotion principle of self-propelled endoscopic capsule.

endoscope's locomotion mechanism. The different movements of five axes are shown with numbers and corresponding arrowhead in Fig. 4(a)–(c). Number 1 with red color indicates magnet assembly's rotation about its longitudinal axis, number 2 with green color shows two magnets' linear motion in opposite direction in the coronal plane, number 3 with blue color represents two magnets' linear motion in opposite direction in the sagittal plane, number 4 with purple color shows the patient support's linear movement in the lateral direction, and number 5 with orange color indicates the patient support's linear movement in the longitudinal direction. By combining movements of five axes in different permutation and sequence, we can navigate magnet built-in capsule endoscope's locomotion through the simulated intestinal tract in multidirections. Four main movements of capsule endoscope are shown in Fig. 4(d), the relative translation between patient support and magnet assembly will steer capsule moving in the lateral or longitudinal direction in terms of patient support's motion path; the opposite motion of magnets in the coronal plane will drive capsule rotating about its vertical axis, this motion changes capsule's orientation, allowing to realize capsule's motion transition from the longitudinal path to the lateral path and *vice versa*. The capsule endoscope is also capable of rotating about its longitudinal axis by pivoting the magnet assembly in the magnet support, this movement is not only useful for adjusting capsule's orientation, but also necessary for enlarging viewing angle of the built-in micro camera to improve diagnosis effect of GI endoscopy.

III. Materials and Methods

A. Fabrication of the Magnet/PMMA Capsule Complex

Fig. 5(a) shows a geometry-optimized magnet/PMMA capsule prototype based on orthogonal process design. The capsule has a diameter of 11 mm, a length of 26 mm, and a weight of 8.82 g. The magnetic shell has a dimension of ø11 mm × ø6 mm × 10 mm, a weight of 6.95 g, and generate a maximum magnetic field of 0.36 T at the external surface.

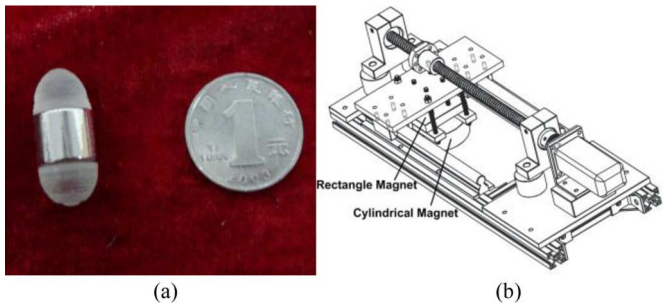

Fig. 5. (a) Geometry-optimized capsule. (b) Schematic of the external magnetic source.

B. External Magnetic-Field Sources

Electromagnets or permanent magnets can be mounted on the magnet assembly of the proposed magnetic propulsion system. In current approach, two groups of permanent Nd–Fe–B magnets are used to provide sufficient magnetic field for driving endoscopic capsule [see Fig. 5(b)]. Each group includes a rectangle Nd–Fe–B magnet and a cylindrical Nd–Fe–B magnet; the rectangle one has a length of 80 mm, a width of 60 mm, a height of 15 mm, and the cylindrical one has a diameter of 90 mm, a height of 30 mm, and generated a field of 0.32 and 0.29 T at the center of its surface, respectively.

C. Simulated Intestinal Tract

Polyvinyl chloride (PVC) tube is used as the simulated intestinal tract for experiments. The length and the diameter of the PVC tube is 1.6 m and 20 mm, respectively. The choice of the simulated intestinal tract is based on the geometry similarity, and the dimension of the chosen PVC tube is approximate to the human's small intestine, which has a typical diameter of 25–30 mm for adults [35].

D. FE Analysis

FE methods are used to simulate magnetic-field distributions and mechanical properties of the proposed magnetic navigation system. Gauss meter (HT100G, HT Magnet Corporation) is used to measure the actual values of generated magnetic field.

E. Pressure Wave of Organ

Nonlinear curve fitting is used for extracting pressure-wave formula based on the *in vivo* measuring results in [36]. The pressure wave turns out to be a Fourier series given by

$$a = A_0 + \sum_{n=1}^{N} [A_n \sin n\omega(t - t_0) + B_n \cos n\omega(t - t_0)], \quad t \geq t_0 \quad (1)$$

where a represents the pressure-wave formula (in kilopascals), and t_0, N, ω, A_0, A_n, and $B_n, n = 1, 2, \ldots, N$, are defined constants.

IV. Modeling

A. Magnetic Propulsion Modeling

In a current free region [37], where

$$\nabla \times \mathbf{H} = 0 \tag{2}$$

it is possible to define the scalar magnetic potential V_m from the relation

$$\mathbf{H} = -\nabla V_m \tag{3}$$

where $\mathbf{H}$ is the magnetic-field intensity.

This is analogous to the definition of the electric potential for static electric fields. Using the constitutive relation between the magnetic-flux density $\mathbf{B}$ and magnetic field density $\mathbf{H}$

$$\mathbf{B} = \mu_0(\mathbf{H} + \mathbf{M}) \tag{4}$$

where μ_0 is the permeability of vacuum, and $\mathbf{M}$ is the magnetization vector, together with the equation

$$\nabla \cdot \mathbf{B} = 0 \tag{5}$$

we can derive an equation for V_m

$$-\nabla \cdot (\mu_0 \nabla V_m - \mu_0 \mathbf{M}) = 0. \tag{6}$$

Along the boundaries far away from the magnet, the magnetic field should be tangential to the boundary as the flow lines should form closed loops around the magnet. The natural boundary condition is

$$\mathbf{n} \cdot (\mu_0 \nabla V_m - \mu_0 \mathbf{M}) = \mathbf{n} \cdot \mathbf{B} = 0 \tag{7}$$

where $\mathbf{n}$ represents the unit normal vector. Thus, the magnetic field is made tangential to the boundary by a Neumann condition on the potential.

Cauchy's equation of continuum mechanics reads

$$\rho \frac{d^2\mathbf{r}}{dt^2} = \nabla \cdot T + \mathbf{f}_{\text{ext}} \tag{8}$$

where ρ is the density, r denotes the coordinates of a material point, T is the stress tensor, and $\mathbf{f}_{\text{ext}}$ is an external volume force. This is the equation solved in the structural mechanics application modes for the special case of a linear elastic material.

In the stationary case (as shown in Fig. 6), there is no acceleration, and the equation representing the force balance is

$$0 = \nabla \cdot T + \mathbf{f}_{\text{ext}}. \tag{9}$$

On the boundary, the following equations apply:

$$\mathbf{n}_1(\bar{T}_2 - T_1) = 0 \tag{10}$$

$$\mathbf{n_1}\bar{T}_2 = \mathbf{n}_1 T_2 + \mathbf{g}_{\text{ext}} \tag{11}$$

where T_1 and T_2 represent the stress tensor in the capsule and the medium around the capsule in the GI tract. The external boundary force $\mathbf{g}_{\text{ext}}$ can represent the reaction force from the wall of the intestine that the capsule is attached to.

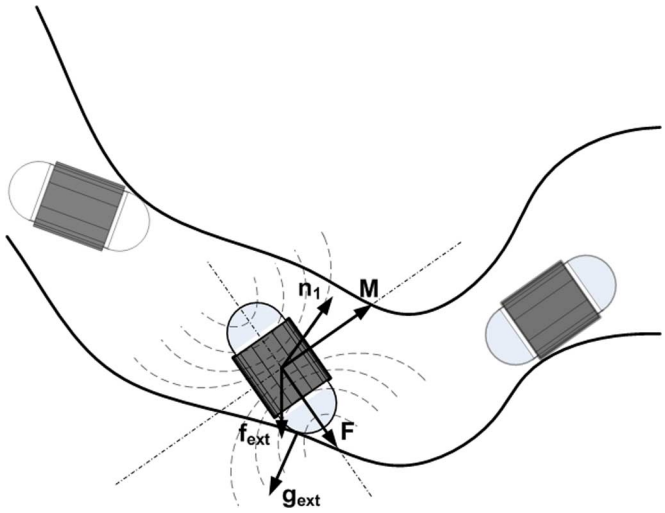

Fig. 6. Illustration of magnetic propulsion modeling.

The equations for the balance of forces on the capsule now become

$$\nabla \cdot T_1 + \mathbf{f}_{\text{ext}} = \mathbf{0} \tag{12}$$

$$\mathbf{n_1}(T_2 - T_1) + \mathbf{g}_{\text{ext}} = \mathbf{0}. \tag{13}$$

For computing the total force $\mathbf{F}$ on the capsule, these equations need to be integrated over the entire capsule and the capsule/medium boundary

$$\int_{\Omega_1} (\nabla \cdot T_1 + \mathbf{f}_{\text{ext}}) dV + \oint_{\partial\Omega_1} (\mathbf{n}_1(T_2 - T_1) + \mathbf{g}_{\text{ext}})\, dS = \mathbf{0}. \tag{14}$$

Now, according to Gauss' theorem

$$\int_{\Omega_1} \nabla \cdot T_1 dV - \oint_{\partial\Omega_1} \mathbf{n}_1 T_1 dS = \mathbf{0}. \tag{15}$$

This means that the external force

$$\mathbf{F}_{\text{ext}} = \int_{\Omega_1} \mathbf{f}_{\text{ext}} dV + \oint_{\partial\Omega_1} \mathbf{g}_{\text{ext}} dS \tag{16}$$

is needed to balance the term for the boundary integral of the stress tensor in the surrounding medium

$$\mathbf{F} = \oint_{\partial\Omega_1} \mathbf{n}_1 T_2 dS \tag{17}$$

to keep the capsule stationary, i.e.,

$$\mathbf{F}_{\text{ext}} + \mathbf{F} = \mathbf{0}. \tag{18}$$

To summarize, the total force $\mathbf{F}$ is computed as a boundary integral of the stress tensor in the medium on the outside of the capsule. Note that to obtain this result, the contribution from the medium pressure gradient has been neglected. This is equivalent to assuming that $\nabla \cdot T_2 = \mathbf{0}$.

Due to limitations of carrying out *in vivo* experiments, simulated intestinal experiments were conducted in cut-open intestine specimen instead of the living body. Therefore, fluidic medium of the intestine is approximated by air. However, in order to estimate the actual stress tensor of the fluidic medium

on the outside of the capsule endoscope, the effect due to the fluidic medium of the intestine should be considered.

For air, the stress tensor [38], [39]

$$T_2 = -pI - \left(\frac{\varepsilon_0}{2}\mathbf{E}\cdot\mathbf{E} + \frac{1}{2\mu_0}\mathbf{B}\cdot\mathbf{B}\right) I + \varepsilon_0 \mathbf{E}\mathbf{E}^{\mathrm{T}} + \frac{1}{\mu_0}\mathbf{B}\mathbf{B}^{\mathrm{T}} \tag{19}$$

where p is the air pressure, ε_0 is the permittivity of vacuum, I is the identity 3×3 tensor (or matrix), and electric field intensity $\mathbf{E}$ and magnetic-flux density $\mathbf{B}$ are 3×1 vectors. In this expression of the stress tensor, air is considered to be nonpolarizable and nonmagnetizable. When air is approximated by vacuum, $p = 0$. This expression of the stress tensor is also known as the Maxwell stress tensor.

Using the fact that, for air, electric flux density $\mathbf{D} = \varepsilon_0\mathbf{E}$ and $\mathbf{B} = \mu_0\mathbf{H}$, the expression for the stress tensor can be written as

$$T_2 = -pI - \left(\frac{1}{2}\mathbf{E}\cdot\mathbf{D} + \frac{1}{2}\mathbf{H}\cdot\mathbf{B}\right) I + \mathbf{E}\mathbf{D}^{\mathrm{T}} + \mathbf{H}\mathbf{B}^{\mathrm{T}}. \tag{20}$$

The equation for the balance of forces becomes

$$\begin{aligned}\mathbf{0} =& \nabla\cdot\left(-pI - \left(\frac{1}{2}\mathbf{E}\cdot\mathbf{D} + \frac{1}{2}\mathbf{H}\cdot\mathbf{B}\right) I\right.\\ &\left. + \mathbf{E}\mathbf{D}^{\mathrm{T}} + \mathbf{H}\mathbf{B}^{\mathrm{T}}\right) + \mathbf{f}_{\mathrm{ext}}.\end{aligned} \tag{21}$$

Consider again the case of a capsule endoscope surrounded by air. To compute the total force, the projection of the stress tensor on the outside of the capsule surface is needed,

$$\begin{aligned}\mathbf{n}_1 T_2 =& -p\mathbf{n}_1 - \left(\frac{1}{2}\mathbf{E}\cdot\mathbf{D} + \frac{1}{2}\mathbf{H}\cdot\mathbf{B}\right)\mathbf{n}_1\\ &+ (\mathbf{n}_1\cdot\mathbf{E})\mathbf{D}^{\mathrm{T}} + (\mathbf{n}_1\cdot\mathbf{H})\mathbf{B}^{\mathrm{T}}\end{aligned} \tag{22}$$

where $\mathbf{n}_1$ is the surface normal, a 1×3 vector, pointing out from the capsule. This expression can be used directly in the boundary integral of the stress tensor for computing the total force $\mathbf{F}$ on the endoscopic capsule.

B. Frictional Resistance Modeling

Given the facts that the power consumption and position control of the endoscopic capsule are largely affected by the frictional resistance of the endoscope inside the GI tract and the viscoelastic characteristics of the internal organs, fundamental understanding of these characteristics is of vital importance; and thus, modeling and simulation of capsule's mechanical locomotion in GI tract are definitely necessary for prediction of frictional forces of the endoscopic capsule moving inside the body [40].

Kim *et al.* established contact mechanics model for analyzing the frictional resistance of a capsule endoscope moving inside the body, as shown in Fig. 7 [40]. For the model development, the following assumptions are made.

1) The GI tract consists of an isotropic material and the small intestine deforms symmetrically toward its radial direction.
2) The volume and the wall thickness of the GI tract are constant.

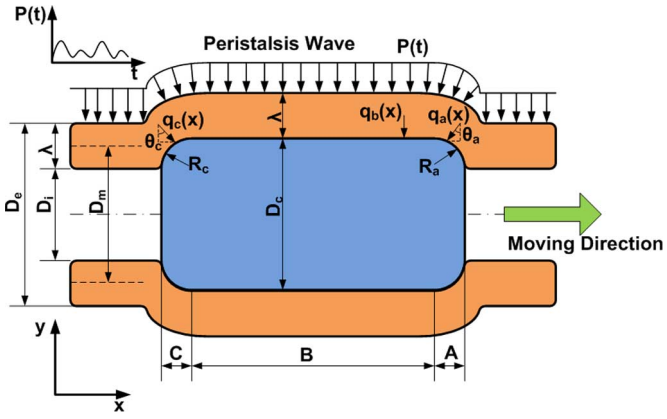

Fig. 7. Frictional resistance modeling of capsule (redrawn based on [40]).

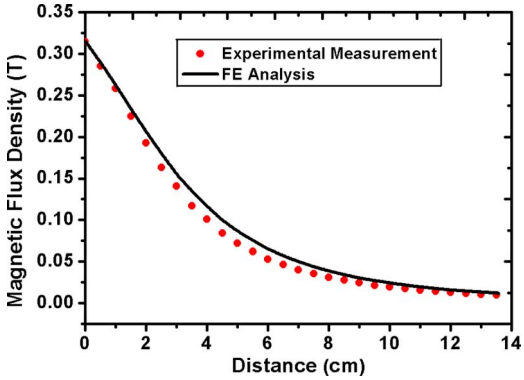

Fig. 8. Magnetic-flux density as a function of distance.

3) The deformed shape of the GI tract is equal to that of the capsule's contact region.
4) There is no inclination of the capsule relative to the axis of the small intestine.

The total frictional force can be expressed as follows [40]:

$$F = F_W + F_V + F_P \tag{23}$$

where F_W is the frictional force related to the capsule weight, F_V is the frictional force induced by the stress due to the viscoelastic deformation of the intestine tract, and F_P is the frictional force induced by the stress due to the pressure of the external organs. The friction component F_P due to the pressure wave is not considered in [40]; however, in case of pressure of external organs, the friction coefficient may be dramatically increased. In the present paper, three major components (F_W, F_V, and F_P) are considered in the FE simulations. FE analysis was performed by using ABAQUS and the results will be discussed in the following.

V. Results and Discussion

Fig. 8 shows the relation between the magnetic-flux density and the distance. The black line plots the simulation results, whereas the circle plots the experiment measurement values. The experimental data match well with the FE analysis, demonstrating that our electromagnetic model is appropriate for analyzing the mechanical properties of the proposed propulsion

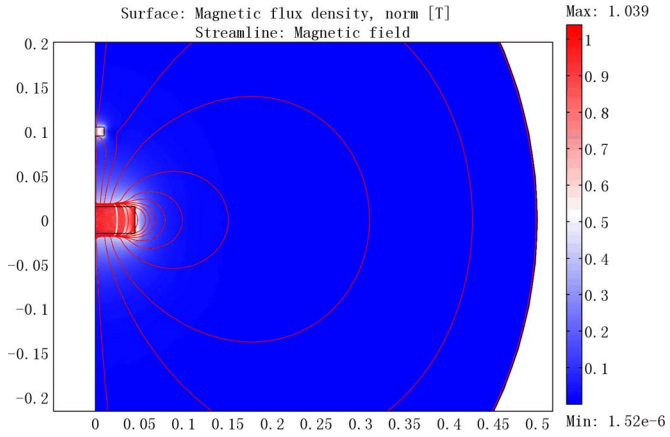

Fig. 9. Visualization of the solved magnetic field.

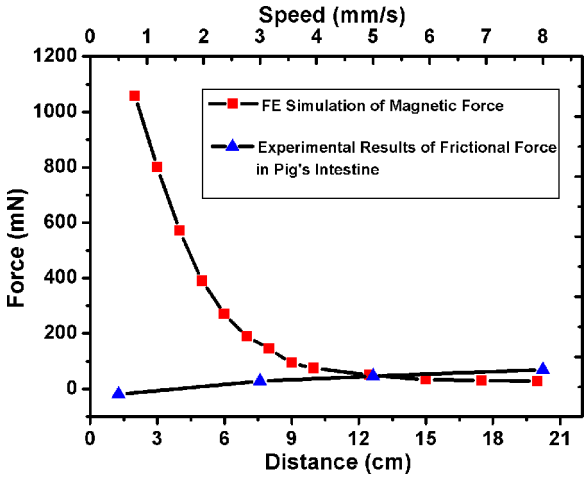

Fig. 10. Comparison between the magnetic force and the friction force (experiment results are from [41]).

system. As we can see, with the increase of the distance between magnetic sources and built-in magnets, the strength of the magnetic-flux density drops rapidly. Thus, tradeoffs between scope of operation area and strength of magnetic field should be considered for providing optimal control parameters of the magnetic propulsion system.

Fig. 9 is a visualization of the solved magnetic field. The streamlines show the lines of magnetic force, and the background color shows the distribution of the magnetic field. The magnetic field is stronger when the magnetic force lines become denser. A maximum intensity of 0.34 T at the surface is obtained. The streamline in the magnetic field maps indicates that the relative orientation between the inner and outer magnets is critical for an accurate and controlled navigation. The appearance of capsule could affect the magnetic circuit. A maximum control force can be obtained when the magnetization plane of the capsule is orthogonal to the surface of the external magnetic sources.

Fig. 10 illustrates the comparison between the magnetic driving force and the frictional resistance force. A square symbol plots the relationships of the distance between external and internal magnets versus the value of magnetic force exerted on the built-in Nd–Fe–B magnets of the magnet/polymethyl methacrylate (PMMA) capsule. The triangle symbol shows the relationships of the capsule's locomotion speed versus the frictional resistance force of the porcine intestine specimen. The frictional resistance force was measured by Wang and Meng through a comprehensive experimental study [41]. There are 15 capsule prototypes, and both closed and open intestine experiments were conducted in Wang's research. We use data of no. 4 in close porcine intestine in terms of three considerations: the dimension of no. 4 capsule prototypes in [41] experiments is same to our capsule (ø11 mm $\times$ 26 mm); the locomotion speed range (0.5–8 mm/s) falls within the control capability of the developed magnetic propulsion system; the status of close intestine is reflected by the FE model and approximates to the practical situation. In order to overcome the frictional resistance of the intestine, the magnitude of distance between external and internal magnets must be adjusted to an appropriate value for generating enough driving force, which can be obtained in terms of square plot line. As we can see, permanent-magnet sources with a surface magnetic-flux density of 0.34–0.5 T is appropriate for driving the magnet/PMMA capsule complex, and the critical distance between the capsule and the external magnetic source is about 12–15 cm. Therefore, operation distance between two groups of magnetic sources can be approximately 24–30 cm. By further optimization of the proposed propulsion system, an operation area with dimensions of 40 cm $\times$ 40 cm can be achieved, which is appropriate for serving the patients with various body conformations (see Table I).

Although the magnetic analysis indicates the feasibilities of the proposed magnetic propulsion system for driving the endoscopic capsule moving inside the intestine, the actual intestinal environment is much more complicated due to the viscoelastic feature, pressure wave of the external organs, and sophisticated surface topography of the intestinal tract. We performed FE simulation by using ABAQUS 6.8 and HYPERMESH 8.0. Viscoelastic characteristics of the intestine, pressure wave, and contact effect between the capsule and the small bowel are considered. In addition, an orthogonal process design with five factors and two levels is carried out for design optimization and analyzing main effects and interaction for frictional force of the capsule's locomotion inside the intestinal tract (parameters and values are listed in Table II). Fig. 11 shows the geometry model of endoscopic capsule's locomotion in the intestinal tract. Five factors—radius of the capsule, radius of curvature, length of the capsule, velocity of the capsule, and frictional coefficient of the intestinal tract are considered for performing the orthogonal process design.

A two-dimension axisymmetric FE model is established for conducting FE analysis. CAX4 H element (four-node bilinear, hybrid with constant pressure) is chosen because it can avoid shear locking and can accurately reflect large deformations due to the contact effect. A contact pair is defined that embodies surface elements of the capsule and the small bowel. The small intestine is defined as the slave surface and the capsule as the master surface in terms of the physical feature of corresponding materials. Stress relaxation material data are based on experimental measurements from [42]. Fig. 12 shows the distributions of von Mises stress that are applied along the capsule of sample

TABLE II
ORTHOGONAL ARRAY OF AVERAGE FORCE UNDER FIVE FACTORS

	R(mm)	ρ(mm)	L(mm)	V(mm/s)	f	Average Force(mN)
Sample1	5.5	1.5	10	0.5	0.2	21.1
Sample2	6	1.5	10	0.2	0.1	19.0
Sample3	5.5	2	10	0.2	0.2	21.1
Sample4	6	2	10	0.5	0.1	21.2
Sample5	5.5	1.5	15	0.5	0.1	14.3
Sample6	6	1.5	15	0.2	0.2	54.9
Sample7	5.5	2	15	0.2	0.1	14.4
Sample8	6	2	15	0.5	0.2	54.8

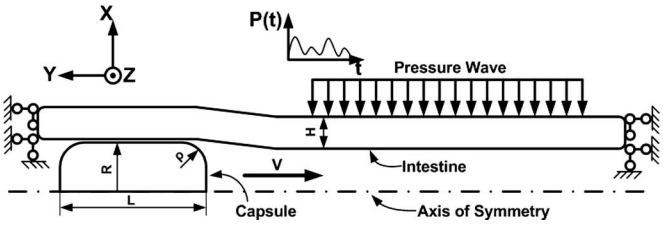

Fig. 11. Geometry model of capsule's locomotion in the intestinal tract.

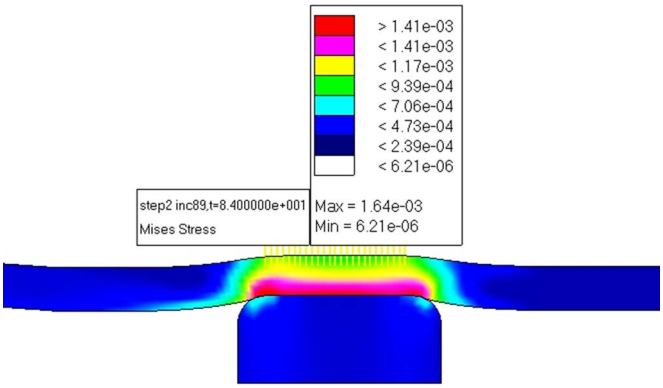

Fig. 12. FE simulations of von Mises stress distributions allied along the capsule moving inside the intestinal tract (in megapascals).

8. Contact effects, pressure wave as well as viscoelastic characteristics can be found. The fitting curve of pressure wave is shown in Fig. 13. Table III summarizes the coefficients in (2). It should be noted that A_0, A_n, and B_n, $n = 1, 2, \ldots, 8$, have a unit of kilopascal. The pressure formula is embodied in the FE simulations.

FE simulations of the frictional force variation of eight samples are shown in Fig. 14. FE results are similar to the experimental measurements from [43], indicating that we can use the FE simulations to obtain important control parameters for the proposed magnetic propulsion system. Scenarios with (samples 1, 3, 5, and 7) and without (samples 2, 4, 6, and 8) pressure-wave action are performed for the purpose of visualizing the effect of the organ pressure wave. The result shows that the resistant force is significantly affected by the external pressure wave; it indicates that design optimization is necessary for a robust control and appropriate propulsion. Based on the FE analysis, an orthogonal process design with five factors and two levels is conducted by using MINITAB 15. Fig. 15 shows the main effects plot for average frictional force of the capsule's locomotion

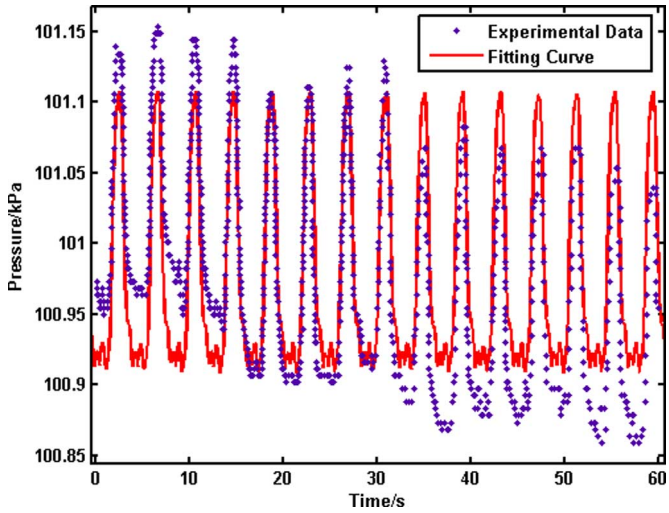

Fig. 13. Fitting curve of the pressure (absolute pressure) of the external organs.

TABLE III
SUMMARY OF COEFFICIENTS

A_0	ω	t_0	N	A_1
0.15	1.545	60	8	-0.07176
B_1	A_2	B_2	A_3	B_3
-0.04983	0.01939	0.03861	-0.002442	-0.01004
A_4	B_4	A_5	B_5	A_6
-0.002647	-0.004526	-0.002789	0.00522	0.005458
B_6	A_7	B_7	A_8	B_8
0.001259	0.0007238	0.002332	-0.0005336	0.001323

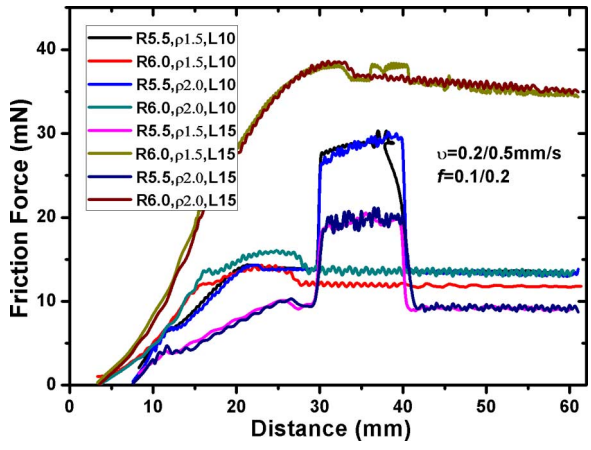

Fig. 14. Frictional force variation of eight samples with different geometric and physical parameters (pressure wave is exerted on the intestinal wall with position of 30–40 mm).

in the intestine. It can be found that the frictional coefficient, the radius of the capsule, and the length of the capsule contribute greatly to the magnitude of the frictional force. With the increase of the frictional coefficient, and the radius and length of the capsule, the frictional resistance force increases significantly. The radius of curvature and the capsule's velocity are

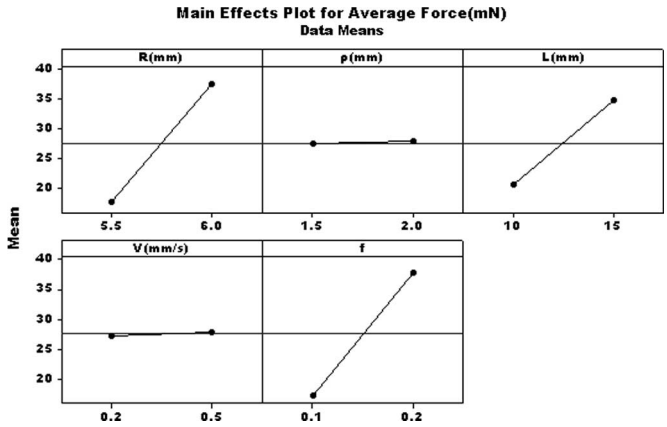

Fig. 15. Main effects analysis of frictional force with five factors.

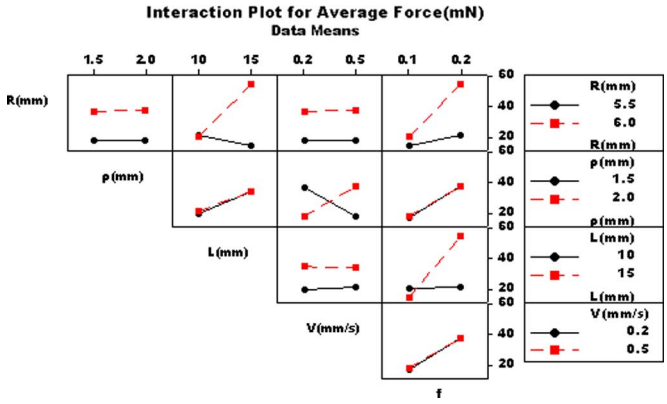

Fig. 16. Interaction effects analysis of frictional force with five factors.

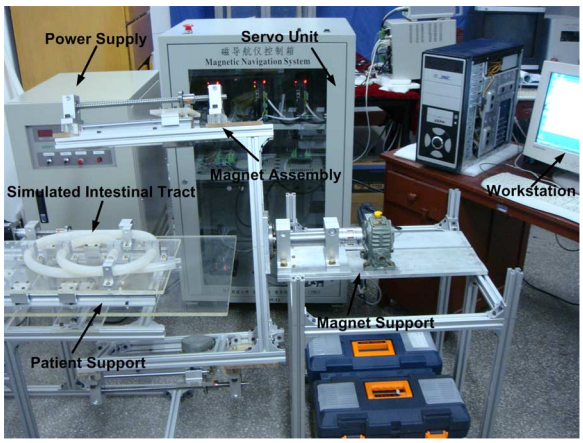

Fig. 17. Magnetic propulsion system for capsule endoscopy.

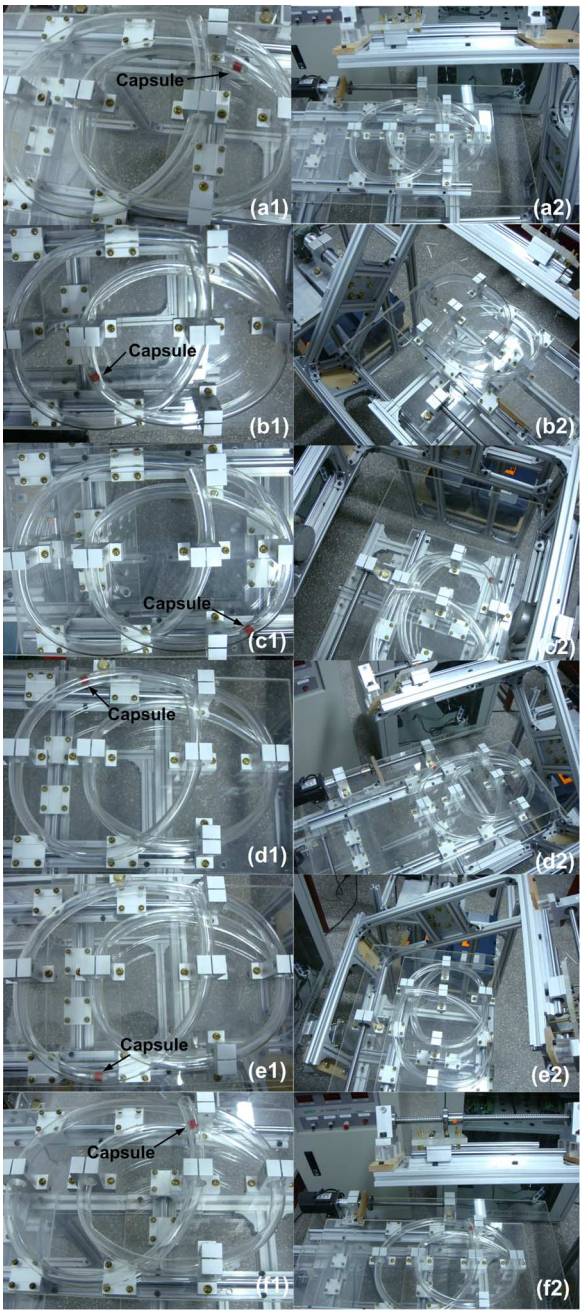

Fig. 18. Movement of the capsule on a simulated intestinal tract.

secondary causes in this case. Fig. 16 indicates the interaction effects of the frictional force of capsule moving inside the small bowel. There are no or little interactions between R and ρ, R and V, ρ and L, ρ and f, L and V, and V and F. However, interactions exist between R and L, R and f, ρ and V, and L and f. We can see that combinations of high frictional coefficient and high radius, or high length result in a great increase of the frictional force. Therefore, design of endoscopic capsule with smaller radius and length as well as suitable surface material that can reduce the frictional coefficient is favorable for reducing the frictional resistance, and thus, facilitating the movement of the endoscopic capsule inside the intestinal tract.

According to the results of the orthogonal process design, a geometry-optimized capsule is fabricated, as shown in Fig. 5(a). A tube-shaped Nd–Fe–B magnet (11 mm ø (6 mm ø) × 10 mm), which is magnetized in the direction of its diameter, is connected with two hemispheroids made of PMMA. The front hemispheroid and the rear one have a radius of 5.5 mm and a radius of curvature of 2 and 1.5 mm, respectively.

Proposed magnetic propulsion system for intestinal endoscopy is developed, as shown in Fig. 17. Experiments of

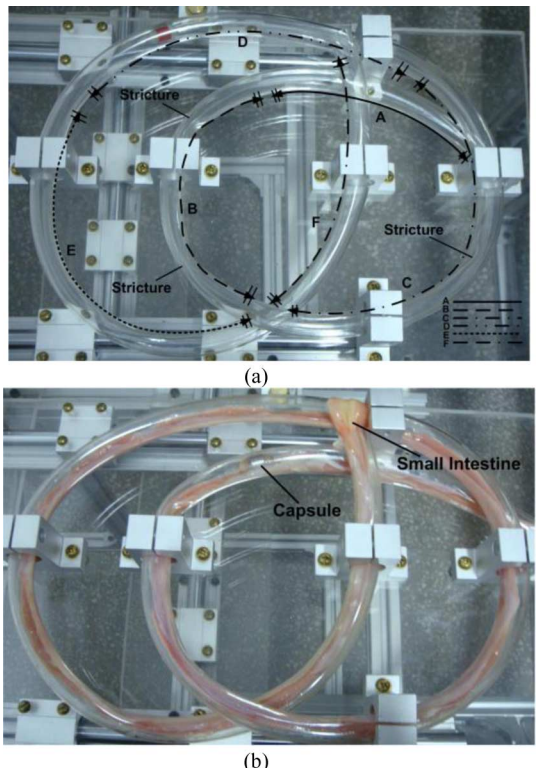

Fig. 19. Simulated intestinal tract (a) PVC tubes. (b) PVC tubes with intestinal layers.

motion control are conducted in a transparent PVC tubes and are presented by the video frames reported in Fig. 18. It shows a combined movement of translation and rotation of the capsule (marked by red color). Due to the visible external manipulation of magnetic navigation system, the capsule can move linearly in both longitudinal and lateral directions, rotate about its longitudinal and lateral axes, and pivot about its vertical axis. Fig. 18(a1)–(f1) shows the location and the moving direction of the capsule at different time in the simulated intestinal tract. The position and orientation of the magnet assembly and the patient support inducing these movements are reported in the related frames Fig. 18(a2)–(f2).

The artificial path was patterned in terms of the tortuous feature of the intestine. *In vitro* experiments are carried out in the transparent PVC tube with and without intestinal layer. The dimension of the simulated intestine is ø20 cm $\times$ 160 cm and it includes six regions, which represent different combination of straight and curved paths (see Fig. 19). Three strictures are set up to simulate the physiological characteristics of the small bowel. Physiological saline is sprayed on the porcine small intestine to avoid drying of the tissue. The locomotion performance of the magnetic propulsion system is recorded for each region of the simulated tract. Table IV summarizes the position and the velocity information of the capsule prototype. The total time of the capsule for going through the 1.6-m-long tract is about 53.09 s for PVC tubes [see Fig. 19(a)] and 148.78 s for intestine [see Fig. 19(b)], respectively. The average velocity is about 30.14 and 10.75 mm/s, respectively.

TABLE IV
SUMMARY OF *IN VITRO* TESTS

Paths	L(cm)	H(mm)	D(cm)	T_P (s)	T_I(s)	V_P (cm/s)	V_I (cm/s)
A	24.4	29	20	2.73	16.2	8.94	1.51
B	21.2	40	16-20	14.9	30.5	1.42	0.70
C	31.5	38	18-20	9.20	41.2	3.43	0.76
D	23.7	34	20	8.35	7.78	2.76	3.05
E	28.7	16	19-20	10.4	37.8	2.76	0.76
F	30.5	55	20	7.51	15.3	4.06	1.99

l, length of the region; *h*, height of the region terminal; *D*, diameter; T_P, time in PVC; T_I, time in intestine; V_P, velocity in PVC; V_L, velocity in intestine.

The proposed approach suggests the feasibilities of steering the endoscopic capsule's location and orientation by the developed magnetic propulsion system. However, further investigations should be carried out for improving the current system in two aspects: 1) external image visualization unit is necessary as the supplementary component of the magnetic propulsion system for providing position information of the capsule. In the current system, eyes serve as the image visualization unit for the servo control unit to perform external manipulation. 2) Fluidic medium of the GI tract and the closed forms of the human body should be taken into consideration for simulating the actual environment of the capsule inside the body cavity under external magnetic equipment.

VI. CONCLUSION

A novel magnetic propulsion system was proposed and manufactured for controlling endoscopic capsule's movements in the intestinal tract. The development of the proposed system was pursued through a combined program of analysis, numerical simulations, and experiments. Locomotion analysis and system design were performed and magnetic-analysis model was established for calculating the magnetic-field distributions and analyzing the mechanical properties of the proposed propulsion system. Based on an orthogonal process design, FE simulations were carried out and a geometry-optimized capsule was fabricated. Simulated intestinal tract experiments were conducted, indicating that the proposed technique is suitable for steering the endoscopic capsule for performing noninvasive GI endoscopy. Further research is currently in progress for visualizing the locomotion control by ways of ultrasonic image.

ACKNOWLEDGMENT

The authors greatly appreciate the help rendered by Dr. D. Xie and Engineer Y. Xu of the School of Mechanical Engineering, Huazhong University of Science and Technology for their help in manufacturing this magnetic propulsion system. The authors also would like to thank Prof. D. Zhang of the California State University for his help in finite-element modeling.

REFERENCES

[1] G. Iddan, G. Meron, A. Glukhovsky, and P. Swain, "Wireless capsule endoscopy," *Nature*, vol. 405, pp. 417–417, May 2000.
[2] M. Hashizume and K. Tsugawa, "Robotic surgery and cancer: the present state, problems and future vision," *Jpn. J. Clin. Oncol.*, vol. 34, pp. 227–237, May 2004.

[3] C. Mc Caffrey, O. Chevalerias, C. O'Mathuna, and K. Twomey, "Swallowable-capsule technology," *IEEE Pervasive Comput.*, vol. 7, no. 1, pp. 23–29, Jan./Mar. 2008.

[4] I. Kassim, W. S. Ng, G. Feng, S. J. Phee, P. Dario, and C. A. Mosse, "Review of locomotion techniques for robotic colonoscopy," in *Proc. 20th IEEE Int. Conf. Robot. Autom. (ICRA)*, Taipei, Taiwan, 2003, pp. 1086–1091.

[5] B. S. Lewis and P. Swain, "Capsule endoscopy in the evaluation of patients with suspected small intestinal bleeding: Results of a pilot study," *Gastrointest. Endosc.*, vol. 56, pp. 349–353, Sep. 2002.

[6] M. Mylonaki, A. Fritscher-Ravens, and P. Swain, "Wireless capsule endoscopy: A comparison with push enteroscopy in patients with gastroscopy and colonoscopy negative gastrointestinal bleeding," *Gut*, vol. 52, pp. 1122–1126, Aug. 2003.

[7] M. Y. Gao, C. Z. Hu, Z. Z. Chen, S. Liu, and H. H. Zhang, "Finite-difference modeling of micromachine for use in gastrointestinal endoscopy," *IEEE Trans. Biomed. Eng.*, vol. 56, no. 10, pp. 2413–2419, Oct. 2009.

[8] A. Menciassi, M. Quirini, and P. Dario, "Microrobotics for future gastrointestinal endoscopy," *Minim. Invasive Ther. Allied Technol.*, vol. 16, pp. 91–100, 2007.

[9] A. Moglia, A. Menciassi, M. O. Schurr, and P. Dario, "Wireless capsule endoscopy: From diagnostic devices to multipurpose robotic systems," *Biomed. Microdevices*, vol. 9, pp. 235–243, Apr. 2007.

[10] M. Delvaux and G. Gay, "Capsule endoscopy: Technique and indications," *Best Pract. Res. Clin. Gastroenterol.*, vol. 22, pp. 813–837, 2008.

[11] T. Nakamura and A. Teran, "Capsule endoscopy: Past, present, and future," *J. Gastroenterol.*, vol. 43, pp. 93–99, 2008.

[12] K. Ishiyama, K. I. Arai, M. Sendoh, and A. Yamazaki, "Spiral-type micromachine for medical applications," in *Proc. Int. Symp. Micromechatron. Human Sci.*, Nagoya, Japan, 2000, pp. 65–69.

[13] M. Sendoh, K. Ishiyama, and K. I. Arai, "Fabrication of magnetic actuator for use in a capsule endoscope," in *Proc. Int. Magn. Conf.*, Boston, MA, 2003, pp. 3232–3234.

[14] A. Yamazaki, M. Sendoh, K. Ishiyama, T. Hayase, and K. I. Arai, "Three-dimensional analysis of swimming properties of a spiral-type magnetic micro-machine," *Sens. Actuators A—Phys.*, vol. 105, pp. 103–108, Jun. 2003.

[15] A. Chiba, M. Sendoh, K. Ishiyama, and K. I. Arai, "Moving of a magnetic actuator for a capsule endoscope in the intestine of a pig," *J. Magn. Soc. Jpn.*, vol. 29, pp. 343–346, 2005.

[16] A. Chiba, M. Sendoh, K. Ishiyama, Y. Suda, K. I. Arai, T. Komaru, and K. Shirato, "Colon endoscope navigation by magnetic actuator and intestine observations," *J. Magn. Soc. Jpn.*, vol. 28, pp. 433–436, 2004.

[17] B. Kim, S. Lee, J. H. Park, and J. O. Park, "Design and fabrication of a locomotive mechanism for capsule-type endoscopes using shape memory alloys (SMAs)," *IEEE-ASME Trans. Mechatron.*, vol. 10, no. 1, pp. 77–86, Feb. 2005.

[18] C. A. Mosse, T. N. Mills, M. N. Appleyard, S. S. Kadirkamanathan, and C. P. Swain, "Electrical stimulation for propelling endoscopes," in *Proc. Digestive Disease Week/101st Annu. Meeting Amer. Gastroenterol. Assoc.*, San Diego, CA, 2000, pp. 79–83.

[19] L. Phee, D. Accoto, A. Menciassi, C. Stefanini, M. C. Carrozza, and P. Dario, "Analysis and development of locomotion devices for the gastrointestinal tract," *IEEE Trans. Biomed. Eng.*, vol. 49, no. 6, pp. 613–616, Jun. 2002.

[20] P. Dario, P. Ciarletta, A. Menciassi, and B. Kim, "Modelling and experimental validation of the locomotion of endoscopic robots in the colon," in *Proc. 8th Int. Symp. Exp. Robot. (ISER 2002)*, Sant Angelo, Italy, pp. 445–453.

[21] A. Menciassi, A. Moglia, S. Gorini, G. Pernorio, C. Stefanini, and P. Dario, "Shape memory alloy clamping devices of a capsule for monitoring tasks in the gastrointestinal tract," *J. Micromech. Microeng.*, vol. 15, pp. 2045–2055, Nov. 2005.

[22] M. Quirini, A. Menciassi, S. Scapellato, C. Stefanini, and P. Dario, "Design and fabrication of a motor legged capsule for the active exploration of the gastrointestinal tract," *IEEE ASME Trans. Mechatron.*, vol. 13, no. 2, pp. 169–179, Apr. 2008.

[23] K. D. Wang, G. Z. Yan, G. Y. Ma, and D. D. Ye, "An earthworm-like robotic endoscope system for human intestine: design, analysis, and experiment," *Ann. Biomed. Eng.*, vol. 37, pp. 210–221, Jan. 2009.

[24] F. Carpi, S. Galbiati, and A. Carpi, "Magnetic shells for gastrointestinal endoscopic capsules as a means to control their motion," *Biomed. Pharmacother.*, vol. 60, pp. 370–374, Sep. 2006.

[25] F. Carpi, S. Galbiati, and A. Carpi, "Controlled navigation of endoscopic capsules: Concept and preliminary experimental investigations," *IEEE Trans. Biomed. Eng.*, vol. 54, no. 11, pp. 2028–2036, Nov. 2007.

[26] F. Carpi and C. Pappone, "Magnetic maneuvering of endoscopic capsules by means of a robotic navigation system," *IEEE Trans. Biomed. Eng.*, vol. 56, no. 5, pp. 1482–1490, May 2009.

[27] J. Peirs, D. Reynaerts, and H. Van Brussel, "Design of miniature parallel manipulators for integration in a self-propelling endoscope," in *Proc. Eurosensors XIII Meeting*, The Hague, Netherlands, 1999, pp. 409–417.

[28] V. R. C. Kode and M. C. Cavusoglu, "Design and characterization of a novel hybrid actuator using shape memory alloy and DC micromotor for minimally invasive surgery applications," in *Proc. 1st IEEE RAS-EMBS Int. Conf. Biomed. Robot. Biomechatron. (BioRob)*, Pisa, Italy, 2006, pp. 455–464.

[29] H. G. Sim, S. K. H. Yip, and C. W. S. Cheng, "Equipment and technology in surgical robotics," *World J. Urol.*, vol. 24, pp. 128–135, Jun. 2006.

[30] D. E. Koditschek, R. J. Full, and M. Buehler, "Mechanical aspects of legged locomotion control," *Arthropod Struct. Dev.*, vol. 33, pp. 251–272, Jul. 2004.

[31] C. Pawashe, S. Floyd, and M. Sitti, "Modeling and experimental characterization of an untethered magnetic micro-robot," in *Proc. 4th Robot. Sci. Syst. Conf.*, Zurich, Switzerland, 2008, pp. 1077–1094.

[32] S. Kumar, I. M. Kassim, and V. K. Asari, "Design of a vision-guided microrobotic colonoscopy system," *Adv. Robot.*, vol. 14, pp. 87–104, 2000.

[33] K. B. Yesin, K. Vollmers, and B. J. Nelson, "Modeling and control of untethered biomicrorobots in a fluidic environment using electromagnetic fields," in *Proc. 9th Int. Symp. Exp. Robot. (ISER)*, Singapore, 2004, pp. 527–536.

[34] New world encyclopedia. (Nov. 10, 2007). [Online]. Available: http://www.newworldencyclopedia.org/entry/Gastrointestinal_tract

[35] Wikipedia. (2006). [Online]. Available: http://en.wikipedia.org/wiki/Small_intestine

[36] S. Park, J. Park, H. Park, S. Park, C. Jee, S. Park, and B. Kim, "Multi-functional capsule endoscope for gastro-intestinal tract," presented at the SICE-ICASE Int. Joint Conf., Busan, Korea, Oct. 2006.

[37] R. P. Feynman, R. B. Leighton, and M. Sands, *The Feynman Lectures on Physics,*. vol. 2, Reading, MA: Addison-Wesley, 1964, ch. 14.

[38] A. Kovetz, *The Principles of Electromagnetic Theory*. Cambridge, U.K.: Cambridge Univ. Press, 1990.

[39] O. Wilson, *Introduction to Theory and Design of Sonar Transducers*. Los Altos, CA: Peninsula, 1988.

[40] J. S. Kim, I. H. Sung, Y. T. Kim, D. E. Kim, and Y. H. Jang, "Analytical model development for the prediction of the frictional resistance of a capsule endoscope inside an intestine," in *Proc. Inst. Mech. Eng. Part H—J. Eng. Med.*, Nov. 2007, vol. 221, pp. 837–845.

[41] X. Wang and M. Q. H. Meng, "An experimental study of resistant properties of the small intestine for an active capsule endoscope," in *Proc. Inst. Mech. Eng. Part H—J. Eng. Med.*, 2010, vol. 224, pp. 107–118.

[42] J. S. Kim, I. H. Sung, Y. T. Kim, E. Y. Kwon, D. E. Kim, and Y. H. Jang, "Experimental investigation of frictional and viscoelastic properties of intestine for microendoscope application," *Tribol. Lett.*, vol. 22, pp. 143–149, May 2006.

[43] N. K. Baek, I. H. Sung, and D. E. Kim, "Frictional resistance characteristics of a capsule inside the intestine for microendoscope design," in *Proc. Inst. Mech. Eng. Part H—J. Eng. Med.*, May 2004, vol. 218, pp. 193–201.

Mingyuan Gao (S'10) was born in Yinchuan, China, in 1985. He received the M.S. degree in mechanical manufacturing and automation from Huazhong University of Science and Technology, Wuhan, China, in 2010.

His current research interests include biomedical equipment, biomechanical modeling, and microsystems packaging.

Mr. Gao received the 2009 GE Foundation TECH Award—first place award.

Chengzhi Hu received the B.S. degree in measuring and control technology and instrumentation and the M.S. degree in mechanical manufacturing and automation from Huazhong University of Science and Technology, Wuhan, China, in 2008 and 2010, respectively. He is currently working toward the Ph.D. degree at Nagoya University, Nagoya, Japan.

His research interests include simulations and analysis of electromagnetics, automation and microrobotics, microsystems packaging technology, and active control of capsule endoscopy.

Zhenzhi Chen received the B.S. degree in mechanical science and engineering from the Harbin Institute of Technology, Harbin, China, in 2008. Since August 2008, he has been working toward the Postgraduate degree at the Institute of Microsystems, Huazhong University of Science and Technology, Wuhan, China.

His research interests include design and modeling for self-propelled robotic endoscopy system.

Honghai Zhang received the Ph.D. degree in mechanical manufacturing engineering from Huazhong University of Science and Technology, Wuhan, China, in 1988.

He is currently a Professor at the National Laboratory for Optoelectronics, Huazhong University of Science and Technology. His research interests include micro/nanomanufacturing technology. He has developed a number of micromanufacturing equipments, such as multifunctionally metrological scanning probe microscopy, nanoimprinting equipment, microjetting platform, and equipment for measurement and control of surface microcharacteristics in precision process.

Sheng Liu (M'93–SM'09) received the B.S. and M.S. degrees from Nanjing University of Aeronautics and Astronautics, Nanjing, China, in 1983 and 1986, respectively, and the Ph.D. degree from Stanford University, Stanford, CA, in 1992.

He is currently with the School of Mechanical Science and Engineering, and the National Laboratory for Optoelectronics, Wuhan, China. His research interests include microsystems (MS)/nano-electromechanical systems (NEMS), LED design and manufacturing, system packaging and integration, reliability, smart materials and composites, and mechanics of materials and structures.

Dr. Liu is a Fellow of the American Society of Mechanical Engineers.